The Astrophysical Journal, 766:80 (8pp), 2013 April 1 doi:10.1088/0004-637X/766/2/80

$H_2(v = 0,1) + C^+(^2P) \rightarrow H+CH^+$ STATE-TO-STATE RATE CONSTANTS FOR CHEMICAL PUMPING MODELS IN ASTROPHYSICAL MEDIA

Alexandre Zanchet[1], B. Godard[2], Niyazi Bulut[1,3], Octavio Roncero[1,5], Philippe Halvick[4], and José Cernicharo[2]
[1] Instituto de Física Fundamental (IFF-CSIC), C.S.I.C., Serrano 123, E-28006 Madrid, Spain; octavio.roncero@csic.es
[2] Centro de Astrobilogía, CSIC-INTA, Torrejón de Ardoz, Madrid, Spain
[3] Department of Physics, Firat University, 23169 Elaziğ, Turkey
[4] Institut des Sciences Moléculaires, Université de Bordeaux, CNRS UMR 5255, 351 cours de la Libération, F-33405 Talence Cedex, France
Received 2012 December 29; accepted 2013 February 7; published 2013 March 11

ABSTRACT

State-to-state rate constants for the title reaction are calculated using the electronic ground state potential energy surface and an accurate quantum wave-packet method. The calculations are performed for H_2 in different rovibrational states, $v = 0$, 1 and $J = 0$ and 1. The simulated reaction cross section for $v = 0$ shows a rather good agreement with the experimental results of Gerlich et al., both with a threshold of 0.36 eV and within the experimental error of 20%. The total reaction rate coefficients simulated for $v = 1$ are two times smaller than those estimated by Hierl et al. from cross sections measured at different temperatures and neglecting the contribution from $v > 1$ with an uncertainty factor of two. Thus, part of the disagreement is attributed to the contributions of $v > 1$. The computed state-to-state rate coefficients are used in our radiative transfer model code applied to the conditions of the Orion Bar photodissociation region, and leads to an increase of the line fluxes of high-J lines of CH^+. This result partially explains the discrepancies previously found with measurements and demonstrates that CH^+ excitation is mostly driven by chemical pumping.

Key words: astrochemistry – molecular data – radiative transfer – scattering

Online-only material: color figures

1. INTRODUCTION

Since the methylidyne cation CH^+ was first discovered in the diffuse interstellar medium (ISM) by Douglas & Herzberg (1941), it has been observed in a variety of interstellar and circumstellar environments. At first, and for nearly 60 years, CH^+ was only detected through its $A^1\Pi - X^1\Sigma^+$ electronic band system observed in absorption toward slightly reddened OB stars (Crane et al. 1995; Gredel 1997; Weselak et al. 2008), thus tracing the diffuse ISM in the solar neighborhood. The *Infrared Space Observatory* (*ISO*; Kessler et al. 1996) and the *Herschel Space Telescope* (Pilbratt et al. 2010) have since broadened the investigation, giving access to the far-infrared rotational spectrum of CH^+ that previously could not be detected from the ground because of the high opacity of the atmosphere. With this new spectral range, CH^+ has now been detected in absorption from the diffuse ISM in the inner Galactic disk (Falgarone et al. 2010; Godard et al. 2012), but also in emission from denser gas in the Orion Bar photodissociation region (PDR; Naylor et al. 2010; Habart et al. 2010), the planetary nebulae NGC 7027 (Cernicharo et al. 1997), and the protoplanetary disk HD 100546 (Thi et al. 2011). One can conclude that the presence of CH^+ is ubiquitous throughout the interstellar matter.

From a theoretical point of view, CH^+ is known to play a key role in the chemistry of the ISM because its hydrogenation leads to the successive formation of two pivot molecular species, the methylene ion CH_2^+ and the methyl cation CH_3^+. On the one hand, CH_2^+ and CH_3^+ are rapidly destroyed by dissociative recombination to form C and CH. Therefore, CH^+ initiates a chemical chain that transforms the ionized carbon into neutral species. This process has been proposed to induce a departure of carbon from the ionization equilibrium (Godard et al. 2009) as suggested by the observations of fine-structure lines in the diffuse ISM (Fitzpatrick & Spitzer 1997) and to regulate the electronic fraction of environments where C^+ is expected to be the dominant ion-carrier. On the other hand, CH_2^+ and CH_3^+ react with O and N to form CO^+, HCO^+, CN^+, HCN^+, and $HCNH^+$, which are the precursors of CO, HCN, HNC, and CN. Hence, CH^+ initiates a chemical chain that leads to the formation of complex molecular species.

The ubiquity of the methylidyne cation is particularly interesting because it raises one of the most resilient puzzles in astrophysics. Since CH^+ is a very reactive ion, its destruction by hydrogenation, hydrogen abstraction, and dissociative recombination are fast processes (McEwan et al. 1999; Larsson & Orel 2008; Mitchell 1990; Plasil et al. 2011). Efficient formation pathways are therefore required to explain its high abundance. Only two chemical reactions may proceed with suitable timescales: the hydrogenation of doubly ionized carbon in environments exposed to a strong X-ray radiation field (Langer 1978), and the hydrogenation of C^+,

$$C^+(^2P) + H_2(v, J) \rightarrow CH^+(v', J') + H, \quad (1)$$

in other Galactic environments. However, since this last reaction is highly endothermic for the vibrational ground state of H_2, with a threshold of ≈0.374 eV (Gerlich et al. 1987), it is unlikely it can proceed at the low temperatures of the diffuse ISM. The puzzle thus consists of finding a suprathermal energy reservoir that may overcome the endothermicity of reaction (1). So far, two scenarios have been invoked: (1) the release of kinetic and magnetic energies induced by low-velocity magnetohydrodynamic shocks (Draine 1986; Pineau des Forêts et al. 1986), Alfvén waves (Federman et al. 1996), turbulent mixing (Xie et al. 1995; Lesaffre et al. 2007), or turbulent dissipation (Falgarone et al. 1995; Joulain et al. 1998; Godard et al. 2009) and (2) the internal energy of vibrationally excited

[5] Corresponding author.

H_2 which greatly enhances the reactivity of reaction (1) (Hierl et al. 1997). While inefficient in the diffuse ISM, this last process has been found to dominate the formation of CH^+, OH, and H_2O in regions where the vibrational levels of H_2 are highly populated by FUV fluorescence, such as the Orion Bar and the hot and dense PDRs of NGC 7027 (Agúndez et al. 2010) and the surface of protoplanetary disks (Thi et al. 2011).

A possibly related issue is the rotational excitation of the far-infrared lines of CH^+ (up to $J = 6$–5) recently observed with *ISO* and the *Herschel*/SPIRE instrument in hot and dense PDRs (Cernicharo et al. 1997; Wesson et al. 2010; Naylor et al. 2010; Habart et al. 2010). Taking into account all the possible excitation sources (i.e., by nonreactive and reactive collisions and by radiative pumping of the rotational, vibrational, and electronic states of CH^+) Godard & Cernicharo (2013) have found that the high-J transitions of CH^+ are dominated by chemical pumping, i.e., by the probability of exciting CH^+ during its chemical formation.

In view of all these observational and theoretical results, the knowledge of the rotationally and vibrationally resolved state-to-state rate constants of reaction (1) is of great interest to improve our understanding of molecular clouds. Up to now, the experimental studies of this reaction (Gerlich et al. 1987; Hierl et al. 1997; Maier 1967; Frees et al. 1979; Mahan & Sloane 1973; Herbst et al. 1975; Harris et al. 1975; Jones et al. 1977; Zamir et al. 1981; Ervin & Armentrout 1986; Glenewinkel-Meyer et al. 1995) have provided information on the integral cross sections and the thermal rate constants and they have been successful in separating the contributions of vibrationally excited H_2 in the levels $v = 0$ and $v = 1$. From the theoretical point of view, several ab initio potential energy surfaces (PESs) have been computed (Liskow et al. 1974; Sakai et al. 1981; Saxon & Liu 1983; Stoecklin & Halvick 2005; Warmbier & Schneider 2011) and many dynamical studies have been performed using quasi-classical trajectories (QCT; Sullivan & Herbst 1978; González et al. 1985) as well as phase space and transition state theory (Truhlar 1969; Chesnavich et al. 1984; Ervin & Armentrout 1986; Gerlich et al. 1987). In addition, the reverse reaction has also been analyzed using QCT (Halvick et al. 2007; Warmbier & Schneider 2011) and a time-independent negative imaginary potential method (Stoecklin & Halvick 2005). However, as far as we know, reaction 1 has never been studied with an exact quantum method.

In this work we investigate the title reaction for the ground and vibrationally excited H_2 using an accurate quantum wave-packet (WP) method, focusing on the state-to-state dynamics to get the corresponding state resolved integral cross sections and rate constants. In the next section we briefly describe the theoretical method used in the simulation and present our results. The applications to astronomical environments are discussed in Section 3, and the conclusions are presented in Section 4.

2. REACTIVE COLLISION SIMULATIONS

In this work we study the state-to-state rate constants for the reaction of Equation (1) with quantum methods and for different initial rovibrational states of H_2. We use the very accurate PES developed by Stoecklin & Halvick (2005) for the electronic ground state of this system, whose main features are shown in Figure 1. The C^++$H_2(v = 0)$ reaction is endothermic by 0.36 eV, becoming exothermic when H_2 is vibrationally excited. This reaction presents an insertion well 4.5 eV deep in a bent geometry.

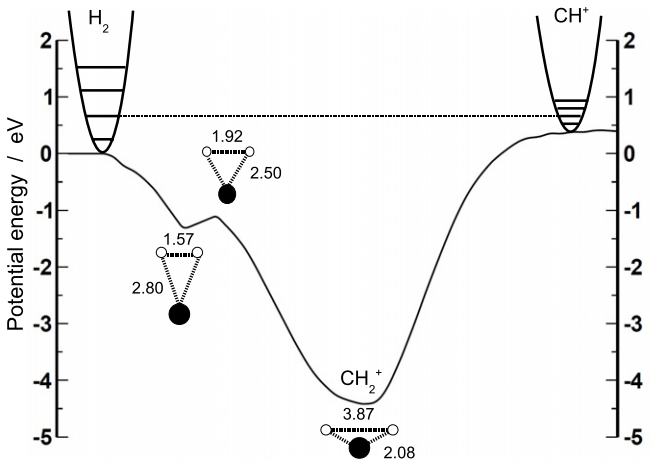

Figure 1. Minimum energy path for the C^++H_2 reaction obtained using the PES of Stoecklin & Halvick (2005).

Table 1
Parameters Used in the Wave Packet Calculations in Reactant Jacobi Coordinates

r_{min} (Å)	0.1
r_{max} (Å)	20
N_r	240
r_{abs} (Å)	16.5
A_r (Å^{-4})	0.001
R_{min} (Å)	0.001
R_{max} (Å)	20
N_R	380
R_{abs} (Å)	16.5
A_R (Å^{-4})	0.0035
N_γ	96 in $[0, \pi/2]$
R_0 (Å)	13
E_0 (eV)	0.33
ΔE (eV)	.186
R'_∞	16
V_{cut} (eV)	3.7
E^ℓ_{cut} (eV)	6.2
Ω_{max}	11
Ω'_{max}	25

Quantum time-independent dynamical calculations of this reaction are difficult to converge because many basis functions are required. Time-dependent WP calculations are better adapted for the purposes of the present work. The propagation in time is done using a modified Chebyshev integrator (Huang et al. 1994; Mandelshtam & Taylor 1995; Huang et al. 1996; Kroes & Neuhauser 1996; Chen & Guo 1996; Gray & Balint-Kurti 1998; González-Lezana et al. 2005) using reactant Jacobi coordinates in a body-fixed frame, which allow one to account for the permutation symmetry of H_2. At each iteration, a transformation to product Jacobi coordinates is done to analyze the final flux on different $CH^+(v', J')$ channels, using an efficient method described by Gómez-Carrasco & Roncero (2006). The MADWAVE3 program has been used for the calculations (Zanchet et al. 2009) and the parameters used in the propagation are listed in Table 1.

The results obtained for zero total angular momentum of the whole triatomic system, $J_t = 0$, are shown in Figure 2. For $v = 0$, the reaction probability manifests a threshold at $\approx$0.36 eV while for $v = 1$ it has no threshold, as expected.

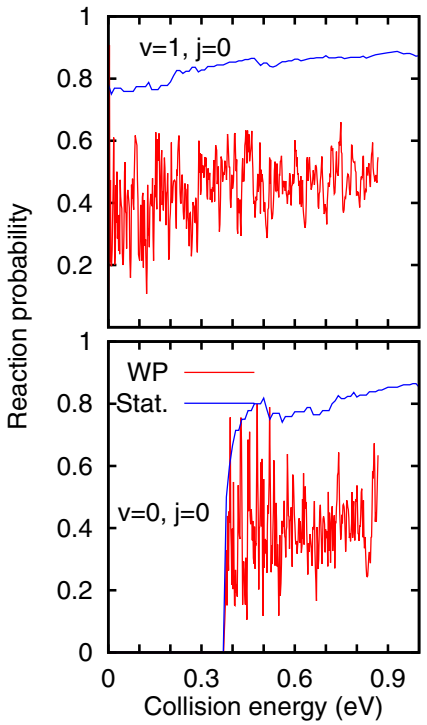

Figure 2. Reaction probability for $J_t = 0$ for the C^++$H_2(v, J = 0)$ for $v = 0$ (bottom panel) and $v = 1$ (top panel) obtained with the quantum wave packet (red) and statistical methods (blue).

(A color version of this figure is available in the online journal.)

In both cases the reaction probability varies between 0.2 and 0.6 with many narrow peaks associated with resonances originating from the deep insertion well. This indicates that the reaction is mediated by these resonances and suggests that the reaction may proceed through a statistical mechanism (Miller 1970; Pechukas & Light 1965).

In order to check this possibility, we have computed the reaction probability for $J_t = 0$ using a simple statistical counting levels scheme in which the probability for each arrangement channel is proportional to the number of accessible product states divided by the sum of all of the states in the three channels (Miller 1970). In Figure 2 the statistical reaction probability is clearly higher than that obtained with the WP method, with the only exception being energies close to the threshold for $v = 0$, where both show an excellent agreement. From this comparison it may be concluded that the reaction is not completely statistical even when it is mediated by resonances. This is probably because of the large mass mismatch between C^+ and H, which requires many collisions within the complex to completely randomize the energy.

The state-to-state integral cross section is obtained in a partial wave expansion as

$$\sigma_{vJ\to v'J'}(E) = \frac{\pi}{(2J+1)k_{vj}^2} \sum_{J_t\Omega\Omega'} (2J_t+1) P^{J_t}_{vJ\Omega\to v'J'\Omega'}(E), \tag{2}$$

where J_t denotes the total angular momentum quantum number and Ω and Ω' are its projections in the reactant and product body-fixed frames, respectively. The total angular momentum with respect to the center of mass of the triatomic system is $\mathbf{J}_t = \mathbf{J} + \mathbf{L}$, where $\mathbf{J}$ is the angular momentum of the BC reagent (described by quantum number J), and $\mathbf{L}$ is the end-over-end angular momentum of atom A with respect to the center of mass of BC. It can also be expressed in terms of the angular momenta of products as $\mathbf{J}_t = \mathbf{J}' + \mathbf{L}'$, since it is conserved along the collision. The state-to-state reaction probabilities, $P^{J_t}_{vJ\Omega\to v'J'\Omega'}(E)$, are simply the square of the collision S-matrix elements and k_{vJ} is the wave vector for the reactants. The sum is over all total angular momenta J_t that contribute to the reaction. As J_t increases, the barrier due to end-over-end rotation also increases, blocking the reaction at energies below the top of the barrier. This is analogous to the increase of the impact parameter in classical mechanics. Here we are interested in collisional energies up to 1.5 eV, which imply an increase of J_t up to ≈120 in Equation (2).

Since the calculation of $P^{J_t}_{vJ\Omega\to v'J'\Omega'}(E)$ for all J_t values is computationally very demanding, the following strategy is used. For $(v = 0, J = 0)$ with a reaction threshold of ≈0.36 eV, the probabilities for $J_t = 0, 5, 10, \ldots, 60$ have been calculated. For $(v = 1, J = 0, 1)$ and $J_t < 22$, the reaction probability has been calculated for all J_t values because the rotational barriers are below the reaction threshold due to the deep well. The rotational barrier introduces a threshold at $J_t = 21$ in the $v = 1, J = 0$ case. Above this J_t value and for $v = 1$, the reaction probabilities shift as J_t increases and only $J_t = 25, 30, \ldots, 60$ have been calculated. For intermediate J_t values, the reaction probabilities are calculated using an interpolation method based on the J-shifting approach (Bowman 1985),

$$P^{J_t}_{vJ\Omega\to v'J'\Omega'}(E) = \frac{J_t - J_1}{J_2 - J_1} P^{J_1}_{vJ\Omega,v'J'\Omega'}(E - E^{J_2} - E^{J_t}) + \frac{J_2 - J_t}{J_2 - J_1} P^{J_2}_{vJ\Omega\to v'J'\Omega'}(E + E^{J_1} - E^{J_t}), \tag{3}$$

where $E^{J_t} = BJ_t(J_t + 1)$ corresponds to the energy shift introduced by the barrier associated with the end-over-end rotation. A value of $B \approx 1$ cm^{-1} is fitted to reproduce the shift of the reaction threshold as J_t increases. In order to check the effect of the interpolation in the $J \in [21, 60]$ interval, the state-to-state cross sections described above have been compared with a second interpolation calculated with a lower number of P^{J_t} P^J for $J_t > 20$, including only $J_t = 21$, 30, 40, 50, and 60. The discrepancy between the two sets of results is less than 1%–3%, and this is taken as the upper bound for the error. For $J_t > 60$, the reaction probabilities have been extrapolated using the J-shifting approach (Bowman 1985), which consists of using the first line in Equation (3) with $J_1 = 60$. The J-shifting extrapolation is known to overestimate the reaction probabilities. However, $P^{J_t=60}$ is only non-zero for energies above 0.5 eV, with a very low probability, <5%. Therefore, when using this $P^{J_t=60}$ to extrapolate, the maximum overestimation error is this 5% for the total reaction probability and only for energies above 0.5 eV.

The vibrationally resolved and total integral cross sections,

$$\sigma_{vJ\to v'}(E) = \sum_{J'} \sigma_{vJ\to v'J'}(E)$$
$$\sigma_{vJ}(E) = \sum_{v'} \sigma_{vJ\to v'}(E), \tag{4}$$

are shown in Figure 3 for $v = 0, J = 0$ (bottom panel) and $v = 1, J = 0, 1$ (top panel). There are six spin-orbit states correlating with $C^+(^2P)$. Neglecting spin-orbit splittings, two

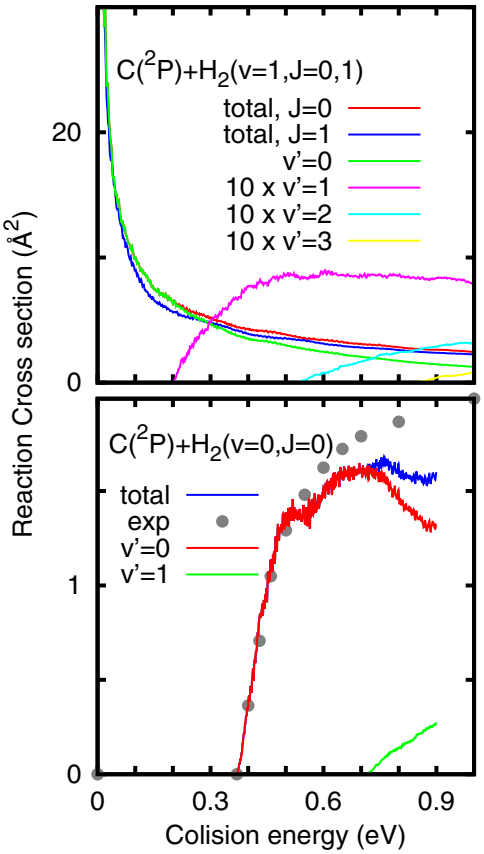

Figure 3. Total and vibrational resolved reaction cross section (in Å^2) as a function of collision energy (in eV) for the C^++$H_2(v, J)$ collisions, obtained with the quantum wave packet method. Bottom panel: for initial $H_2(v = 0, J = 0)$. Top panel for $H_2(v = 1, J = 0$ and 1). For $v = 0$ the experimental values are taken from Gerlich et al. (1987). The simulated cross sections have been multiplied by the electronic partition function, $Q_e(T)$, at 300 K ($Q_e = 0.407$).
(A color version of this figure is available in the online journal.)

of these states correlate with the $CH^+(^1\Sigma^+)$+$H(^2S)$ asymptote (Sakai et al. 1981), giving rise to the electronic partition function $Q_e = 1/3$. If we consider instead the spin-orbit splitting of 63.4 cm^{-1} = 91.2 K between the $^2P_{1/2}$ and $^2P_{3/2}$ states, the electronic partition function is given by

$$Q_e(T) = \frac{2}{2 + 4e^{-91.2/T}}. \quad (5)$$

Assuming that the electronic ground PESs correspond to the two $C^+(^2P_{1/2})$ states, while the four $C^+(^2P_{3/2})$ states are not reactive at all, the cross section of Equation (2) must be multiplied by Q_e, which is 0.407 at the experimental temperature of 300 K (Gerlich et al. 1987).

For $v = 0$, the experimental values of Gerlich et al. (1987) are also shown. These experimental values correspond to the trial function points used to describe crossed beam measurements of a relative cross section with a typical error of 20%. The simulated cross section for collision energies below 0.53 eV is in very good agreement with the experimental value, showing a very similar increasing behavior at the threshold, especially for $Q_e = 0.407$. For higher energies, however, the theoretical values are significantly lower. This is attributed to two possible reasons. The first is the experimental error. The measurements were obtained in relative units and then scaled to reproduce the phase space results obtained by Gerlich et al. (1987) with a typical error of 20% (Gerlich et al. 1987). The second reason is that these measurements correspond to a temperature of 300 K involving several rotational states of H_2 (Gerlich et al. 1987).

Experiments were performed at different temperatures (Ervin & Armentrout 1986; Gerlich et al. 1987; Hierl et al. 1997), and state-specific rate coefficients were determined by numerical integration of the measured cross sections. The researchers obtained good agreement using Arrhenius-type functions for describing state-specific rate constants, and found that they properly fit phase space theory results (Ervin & Armentrout 1986; Gerlich et al. 1987). It was found (Ervin & Armentrout 1986; Gerlich et al. 1987; Hierl et al. 1997) that the state-specific rate coefficients increase as the initial rotational excitation of H_2, J increases as a result of the higher total energy. Thus, considering that the experimental results correspond to a mixture of rotational states of H_2, they are expected to be larger than those corresponding to simply $J = 0$, as considered here in Figure 3. For all these reasons we may conclude that the simulated cross section for $v = 0$ is reasonably accurate.

For $v = 1$ in the top panel of Figure 3, there is no threshold to form $CH^+(v' = 0)$ products and the cross section increases as collision energy decreases, as expected in exothermic reactions. For $CH^+(v' > 0)$, however, the reaction presents thresholds and considerably lower cross sections. The $\sigma_{v=1\rightarrow v'=0}$ cross sections are several orders of magnitude larger than in any other case, especially at low collision energies, so it is expected to have a significant contribution to the formation of CH^+ molecules in the ISM, even when vibrationally excited $H_2(v = 1)$ has a low abundance.

The results obtained for $v = 1$, $J = 0$ and 1 in the top panel of Figure 3 are rather similar. In fact, for $J = 1$ they are slightly lower, which is explained by rotational disruption, i.e., the rotational excitation somehow inhibits the reaction and/or the formation of the CH_2^+ complex. This behavior is more remarkable in reactions with barriers (González-Sánchez et al. 2011), followed by an increase of the cross sections when the rotational excitation increases even more. For this reaction with no threshold, however, it is expected that initial rotation had a minor effect. Also, since the reaction is mediated by long-lived resonances, it is reasonable that the memory of the initial state was lost after some vibrations of the complex. This invariance of the cross section with rotation for $v = 1$ is in contrast to the increase reported for $v = 0$. However, this apparent contradiction vanishes when we take into account that the endothermic reaction for $v = 0$ becomes exothermic for $v = 1$.

In order to get the rate coefficients, attention must be paid to low collision energies, $E < 0.01$ eV, where WP methods present inaccuracies, especially due to the application of absorbing potentials allowing one to use finite grids. In the case of ion–molecule reactions showing no barrier in the PESs, the reaction cross sections are usually estimated by the Langevin capture theory (Langevin 1905; Gioumousis & Stevenson 1958), which predicts that the cross section decays as $E^{-1/2}$. The analysis of the flux over all rearrangement channels allows us to conclude that the WP calculations are accurate down to collision energies of 0.03 eV. At this energy we fit the exothermic state-to-state cross sections, $\sigma_{vJ\rightarrow v'J'}(E)$, to the Langevin behavior, $AE^{-1/2}$, having only one parameter as applied recently to study the H^++LiH exothermic reaction (Aslan et al. 2012). This is done for $J' \leqslant 8$, since for higher rotational excitation of the products the reaction has a threshold and it is therefore free from this inaccuracy.

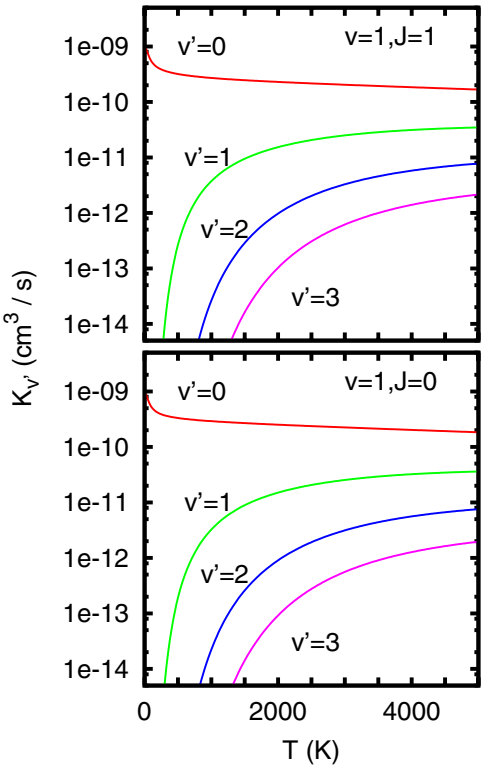

Figure 4. Vibrationally resolved rate constants for the C^++H_2(v = 1, J = 0,1)→ CH(v')+H, summing over all final rotational states obtained by numerical integration of the cross section.

(A color version of this figure is available in the online journal.)

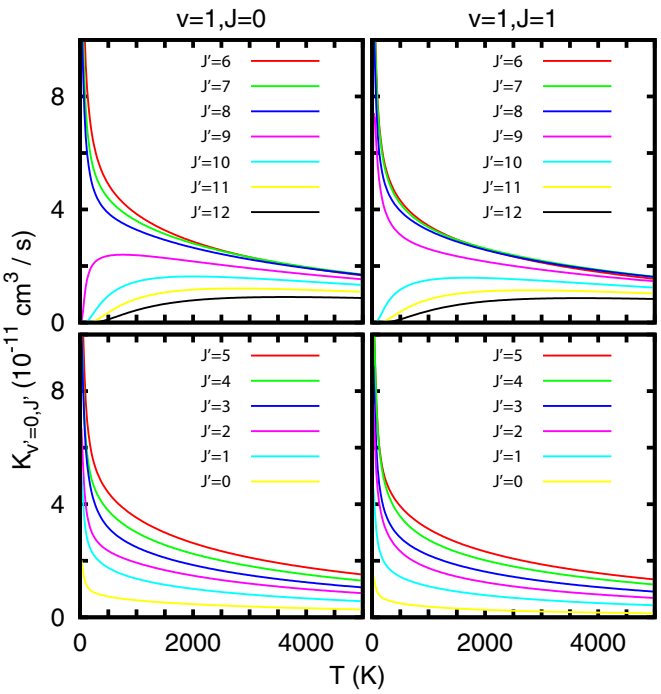

Figure 5. Rotationally resolved rate constants for the C^++H_2($v = 1, J = 0,1$)→ CH($v' = 0$, J')+H.

(A color version of this figure is available in the online journal.)

The state-to-state rate coefficients are then obtained by numerical integration over the collisional energy as

$$K(v, J, v', J')(T) = \left[\frac{8}{\pi\mu\,(k_B T)^3}\right]^{1/2} Q_e(T) \times \int_0^\infty E\,\sigma_{vJ\to v'J'}(E) e^{-E/k_B T}\,dE, \quad (6)$$

where μ is the $C^+ + H_2$ reduced mass. The vibrationally resolved rate constants are shown in Figure 4 for $v = 1$ and $J = 0$ and 1. As described above, the initial rotational excitation has no significant effect on the rates, at least for $J = 1$. For the excited vibrational states the rates show an increase at low temperatures, as expected by the existence of a threshold, but they are essentially negligible in all the temperature ranges considered.

The total rate thus obtained for $v = 1$ is 3×10^{-10} cm^3 s^{-1} at 800 K and it decreases slowly as temperature increases. This value is about three times smaller than the experimental value estimated by Hierl et al. (1997), 1–2×10^{-9} cm^3 s^{-1}. These authors estimated an uncertainty factor of two for this value essentially due to the small difference data used to extract the rates. In their derivation, the cross sections at different temperatures were fitted by a sum of vibrational contributions as described above for rotation but with the rotational effect of reagents included. Considering this uncertainty factor of two, the simulated rates in this work are lower than the experimentally estimated one by a factor of between 1 and 2. Because of the high experimental uncertainty it would be desirable to have new and more accurate measurements. Also, the accuracy of the simulated value has to be addressed. Due to the relatively high accuracy of the dynamical calculations performed here, we consider that the main source of error might be the PESs. One crucial issue at this point is the height of the barrier or, in this case, the endothermicity of the reaction. However, this value seems to be rather accurate since the experimental threshold is well reproduced. Apart from details of the PESs, the possible origin of theoretical error is the use of a single surface to describe the reaction. It is worth mentioning that the electronic partition factor is about 0.36 at 800 K. Thus any contribution coming from the two (or four including spin-orbit couplings) excited electronic states may be significant. Since the two excited electronic states seem to have a very high barrier, the occurrence of non-adiabatic transitions must be examined. To conclude, we consider that the simulated values reported in this work are rather accurate, with an uncertainty, although difficult to estimate, less than a factor of two.

The individual state-to-state rate constants, $K_{v=0J=0,1\to v'=0J'}(T)$, are shown in Figure 5 ($J = 0$ left panels, $J = 1$ in right panels). It should be noted that not all J' rotational channels of CH^+ products are open. Thus, for $v = 1$, $J = 0$, only $CH^+(J')$ with J' <9 are open, while the rest present a threshold. For $v = 1$, $J = 1$, the increase of total energy due to the rotational excitation of H_2 reactants shifts the threshold to $J' = 10$. In the cases of no threshold, the increase as T tends toward zero is due to the fast variation of the electronic partition function since the Langevin extrapolation performed in those cases would yield a constant value of the rate coefficients. For $J' \geqslant 9(10)$, apart from the change of the threshold, the rotational excitation of H_2 has only a small effect. The rates show an increase with increasing J', up to a maximum at $J' = 5$–6 and then a monotonous decrease for all the temperatures analyzed. Most final products are formed in $v' = 0$ and $J' \in [4 - 9]$.

3. IMPLICATIONS FOR THE MODELING OF ASTRONOMICAL SOURCES

The quantum description of the reaction $C^+ + H_2(v, J) \rightarrow CH^+(v', J') + H$ may have two major impacts on the modeling and understanding of molecular clouds.

1. It provides new rates for the total production of CH^+ depending on the distribution of H_2 among its rovibrational levels. Consequently, it may alter our understanding of the global formation process of CH^+ and modify the abundances predicted by chemical models.
2. The analysis of the main excitation pathways of CH^+ performed by Godard & Cernicharo (2013) shows that the distribution of CH^+ among its rotational levels is mostly driven by chemical pumping, i.e., by its chemical formation in excited states. Therefore, the state-to-state rate constants computed in this paper could have a significant impact on the excitation of the rotational transitions of CH^+ predicted by radiative transfer models. Since molecular lines are used as diagnostics of the physical conditions of the interstellar matter, the aftermaths extend to the density and the temperature inferred from the infrared emission lines of CH^+ detected in hot and dense PDRs (Cernicharo et al. 1997; Wesson et al. 2010; Naylor et al. 2010; Habart et al. 2010) and in protoplanetary disks (Thi et al. 2011).

In the following, we thus discuss the implications of our calculations on the chemistry and the excitation mechanisms of CH^+ in several astronomical environments.

3.1. Total Formation Rate of CH^+

As shown in the previous section, the comparison of the present calculations with the existing experimental studies reveals some inconsistencies. On the one hand, the reaction cross section of C^+ with $H_2(v = 0, J = 0)$ is about 30% smaller than the one measured by Gerlich et al. (1987) in the high collision energy limit ($E \geqslant 0.9$ eV). Since the experimental values include the contributions of higher rotational states of H_2 the disagreement is probably smaller, especially taking into account the estimated experimental error of ≈20%. On the other hand, the total reaction rate of C^+ with $H_2(v = 1)$ is two times smaller than the values measured by Hierl et al. (1997) and five times smaller than the Langevin collision rate.

Adopting the latter for the reaction between C^+ and $H_2(v = 1)$, Agúndez et al. (2010) found that the fraction of vibrationally excited H_2 in the diffuse ISM is too low ($<10^{-7}$) to significantly affect the total column density of CH^+ predicted by PDR-type models. A similar result was recently obtained by Lesaffre et al. (2013) who found that including the formation of CH^+ via the vibrational levels of H_2 increases the abundance of CH^+ predicted by high-velocity shock models (shock velocity $\geqslant$ 20 km s^{-1}) by less than a factor of two. It is concluded that the formation of CH^+ in diffuse gas predominantly occurs through the vibrational ground state of H_2. We therefore estimate that adopting our data in chemical codes instead of the values given by Gerlich et al. (1987) would decrease the amount of CH^+ produced in the chemical models of the diffuse ISM by less than 30%.

The effects of our calculations are more substantial in regions where CH^+ originates from vibrationally excited H_2, such as the hot and dense PDRs and the surface of protoplanetary disks (Agúndez et al. 2010; Thi et al. 2011). In this case, we predict that the state-to-state rate constants computed in this paper would reduce the total column density of CH^+ by about a factor of five. Interestingly, in such astronomical environments illuminated by a strong FUV radiation field, CH^+ is mainly destroyed via collisions with atomic hydrogen. The reduction in CH^+ abundances may thus be balanced by adopting the recent experimental results of Plasil et al. (2011), who showed that the destruction rate of $CH^+(J = 0)$ by reactive collisions with H is two to three times lower than that of rotationally excited CH^+ at low kinetic temperatures ($T < 60$ K). Since CH^+ mostly lies in its ground rotational state, the global destruction rate could be considerably reduced. Unfortunately, the state-specific rates of the $CH^+ + H$ reaction have never been measured in the high temperature domain ($T \sim 1000$ K) where CH^+ is expected to be formed.

3.2. Excitation of the Rotational Lines of CH^+

To estimate the impact of the state-to-state chemistry on the rotational excitation of CH^+ we have computed its steady-state level populations using the MADEX (MADrid molecular spectroscopy EXcitation) excitation code (Cernicharo 2012), a radiative transfer model based on the multi-shell large velocity gradients formalism (Goldreich & Kwan 1974), and a molecular spectroscopic database. The nonreactive collisions of CH^+ with e^- were found to pilot the distribution of CH^+ among the low-J rotational levels, and to even compete with the chemical pumping in the excitation of the high-J transitions in C-rich environments (e.g., NGC 7027, Godard & Cernicharo 2013). To maximize the effect of chemical pumping, we therefore consider here a prototypical hot and dense PDR with standard elemental abundances and strong constraints on its geometry and total column density: the Orion Bar (e.g., Hogerheijde et al. 1995; Young Owl et al. 2000; Walmsley et al. 2000; Pellegrini et al. 2009; Arab et al. 2012).

As in Godard & Cernicharo (2013), the interclump medium of the Orion Bar is modeled as a homogeneous PDR of density $n_H = 5 \times 10^4$ (Young Owl et al. 2000), illuminated by a UV radiation field of $\sim 3 \times 10^4$ that of the local ISRF (Marconi et al. 1998). Its kinetic temperature profile and chemical composition as functions of the distance from the ionization front (see Figure 5 of Godard & Cernicharo 2013) are computed with the Meudon PDR code, a one-dimensional chemical model in which a static slab of gas of given thickness is illuminated on one side or on both sides by a given FUV radiation field (Le Petit et al. 2006). By adopting the CH^+ abundances computed with the Meudon PDR code, we deliberately neglect the role of the state-to-state rate constants on the chemistry of CH^+ and solely focus here on their effects on the rotational excitation.

With all these physical and chemical properties we ran MADEX in three different configurations: (1) considering only the excitation by nonreactive collisions, (2) including chemical pumping and assuming that the probability to form CH^+ in an excited level follows a Boltzmann distribution at the kinetic temperature of the gas (based on the prescription of Black 1998 and van der Tak et al. 2007), and (3) adopting the branching ratios obtained with our quantum calculations. In the latter case, the state-specific rates for the formation of $CH^+(v', J')$ via $C^+ + H_2(v = 1, J = 0)$ were fitted with the function $C(v', J') \times 0.9998^T \times \exp[(5157 + E(v', J') - E(v = 1, J = 0))/T]$ where $E(v', J')$ is the energy of the rovibrational level of CH^+ and $E(v = 1, J = 0)$ is the energy of the $v = 1, J = 0$ level of H_2. The same functional form and the same constants $C(v', J')$ were then used to describe the state-specific rates of the reaction $C^+ + H_2(v \geqslant 1, J)$. If not entirely justified, this assumption is

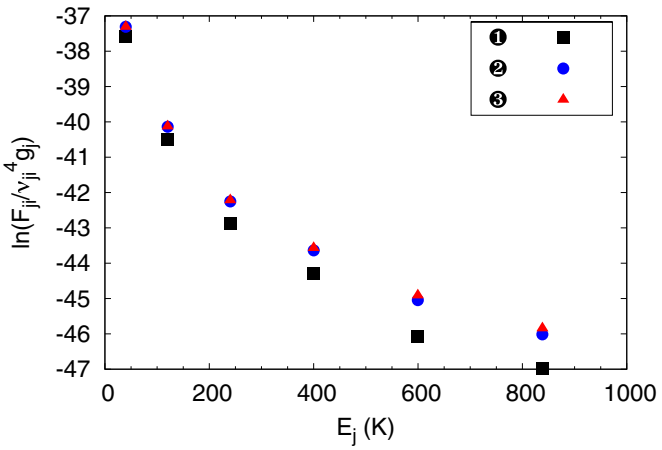

Figure 6. CH^+ rotation diagram in the Orion Bar PDR predicted by the MADEX excitation code in configurations (1), (2), and (3) (see the main text). On the y-axis, we display the variable $\ln(F_{ji}/\nu_{ji}^4 g_j)$, where F_{ji} is the line flux in W m^{-2}, ν_{ji} is the frequency of the transition in THz, and g_j is the statistical weight of the upper level j.

(A color version of this figure is available in the online journal.)

nonetheless supported by the similarity of $K(v, J, v', J')(T)$ computed for $H_2(v = 1, J = 0)$ and $H_2(v = 1, J = 1)$ (see Figures 4 and 5). The resulting beam-averaged continuum-subtracted intensities of the first six rotational lines of CH^+ are shown in Figure 6 as functions of the energy of the upper levels.

The comparison of models (1), (2), and (3) confirms the importance of chemical pumping to the excitation of all the rotational lines of CH^+. In particular, the $J \geqslant 3$–2 transitions appear to be mostly driven by chemical formation, as was already revealed by Godard & Cernicharo (2013). In addition, we find that adopting the state-specific rates for the production of CH^+ has a substantial impact on the distribution of the molecule among its rotational levels: while marginal (<5%) for the low-J rotational lines, it increases the line fluxes of the $J = 4$–3, $J = 5$–4, and $J = 6$–5 transitions by 7%, 15%, and 20%, respectively. This result only partly explains the discrepancy observed between the emission intensities of the $J = 5$–4 and $J = 6$–5 transitions predicted with MADEX in NGC 7027 (Godard & Cernicharo 2013) and those measured with *ISO* (Cernicharo et al. 1997). However, since the internal energy of H_2 is found to favor the excitation of high J lines, our choice to adopt the same chemical rate functions for all the reactions $C^+ + H_2(v \geqslant 1, J)$ may underestimate their actual rate constants. Additional WP calculations involving higher states of H_2 are therefore required to obtain a more reliable prediction of the excitation of CH^+ in interstellar and circumstellar media. These calculations are in progress and will be presented in a forthcoming paper.

4. CONCLUSIONS

We have performed accurate quantum calculations of the reaction rates of $C^+(^2P) + H_2(v = 0, 1, J = 0, 1) \rightarrow CH^+(v', J') + H$ using a single PES and a quantum WP method. The rates have been computed for all rovibrational levels of CH^+ up to $v' = 3$ and $J' = 40$ and as functions of the kinetic temperature up to $T = 5000$ K, thus encompassing the physical conditions of astronomical environments where CH^+ is expected to be formed.

The reaction between C^+ and the rovibrational ground state of H_2 is highly endothermic and its calculated cross sections are in excellent agreement with those inferred from previous experimental studies. In contrast, the reaction rates of $C^+ + H_2(v = 1)$ are found to be about two times smaller than the experimental values. The analysis of the state-to-state chemical rates of $C^+ + H_2(v = 1, J)$ reveals the variations of the reactivity of the system depending on the internal energy of the reactants and products. We find that the rates are adequately reproduced by adopting an Arrhenius-type exponential cutoff with an energy barrier, $\sim 5157\,\mathrm{K} + E' - E$, where E' and E are the internal energies of CH^+ and H_2, respectively. In addition, the reaction rate constants are found to be maximal for $CH^+(J' = 6)$ in the entire temperature domain.

These theoretical investigations have substantial impacts on the modeling of astronomical sources with state-of-the-art chemical and radiative transfer models and provides new insights for the interpretations of the rotational transitions of CH^+ recently observed with *ISO* and the *Herschel Space Telescope*. In particular, we found that including the detailed state-to-state rates in excitation models increases the intensities of the high J rotational emission lines of CH^+ in astronomical regions where the excitation of CH^+ is mostly driven by chemical pumping. This result partly explains the discrepancies found between the fluxes of the $J = 5$–4 and $J = 6$–5 transitions of CH^+ observed toward NGC 7027 and those predicted by the radiative transfer model.

Given the importance of the internal energy of H_2 in the reactivity of the title reaction, additional calculations involving higher rovibrational states of H_2 are required. The comparison of the rates obtained for $H_2(v = 1, J = 0)$ and $H_2(v = 1, J = 1)$ shows no significant deviations. This is due to the fact that the reaction proceeds through the formation of the CH_2^+ complex—in which the memory of the initial state is lost—and to the low extra energy injected in the system by only increasing the rotational quantum number of H_2 from 0 to 1 (15 meV). For all these reasons, we are currently investigating the effect of the $v > 1$ vibrational states of H_2.

We want to acknowledge Professor F. J. Aoiz for fruitful discussion. N.B. acknowledges the Higher Educational Council of Turkey for a visiting scholarship and TUBITAK for TR-Grid facilities. This work has been supported by the program CONSOLIDER-INGENIO 2010 of the Ministerio de Ciencia e Innovación under grant CSD2009-00038, entitled "Molecular Astrophysics: the Herschel and Alma era," and by grant No. FIS2010-18132, and by Comunidad Autónoma de Madrid (CAM) under grant No. S-2009/MAT/1467. The calculations have been performed in the parallel facilities at the CESGA computing center through ICTS grants, which are acknowledged.

REFERENCES

Agúndez, M., Goicoechea, J. R., Cernicharo, J., Faure, A., & Roueff, E. 2010, ApJ, 713, 662
Arab, H., Abergel, A., Habart, E., et al. 2012, A&A, 541, A19
Aslan, E., Bulut, N., Castillo, J. F., et al. 2012, ApJ, 759, 31
Black, J. H. 1998, FaDi, 109, 257
Bowman, J. M. 1985, AdChP, 61, 115
Cernicharo, J. 2012, in Proc. ECLA-2011: Proceedings of the European Conference on Laboratory Astrophysics, ed. C. Stehlé, C. Joblin, & L. d'Hendecourt (EAS Publications Series; Cambridge: Cambridge Univ. Press)
Cernicharo, J., Liu, X.-W., Gonzalez-Alfonso, E., et al. 1997, ApJL, 483, L65
Chen, R., & Guo, H. 1996, JChPh, 105, 3569
Chesnavich, W. J., Akin, V. E., & Webb, D. A. 1984, ApJ, 287, 676
Crane, P., Lambert, D. L., & Sheffer, Y. 1995, ApJS, 99, 107
Douglas, A. E., & Herzberg, G. 1941, ApJ, 94, 381
Draine, B. T. 1986, ApJ, 310, 408

Ervin, K. M., & Armentrout, P. B. 1986, JChPh, 84, 6738
Falgarone, E., Godard, B., Cernicharo, J., et al. 2010, A&A, 521, L15
Falgarone, E., Pineau des Forêts, G., & Roueff, E. 1995, A&A, 300, 870
Federman, S. R., Rawlings, J. M. C., Taylor, S. D., & Williams, D. A. 1996, MNRAS, 279, L41
Fitzpatrick, E. L., & Spitzer, L., Jr. 1997, ApJ, 475, 623
Frees, L. C., Pearl, P. L., & Koski, W. S. 1979, CPL, 63, 108
Gerlich, D., Disch, R., & Scherbarth, S. 1987, JChPh, 87, 350
Gioumousis, G., & Stevenson, D. P. 1958, JChPh, 29, 294
Glenewinkel-Meyer, T., Hoppe, U., Kowalski, A., Ottinger, C., & Rabenda, D. 1995, IJMSI, 144, 167
Godard, B., & Cernicharo, J. 2013, A&A, 550, A8
Godard, B., Falgarone, E., Gerin, M., et al. 2012, A&A, 540, A87
Godard, B., Falgarone, E., & Pineau Des Forêts, G. 2009, A&A, 495, 847
Goldreich, P., & Kwan, J. 1974, ApJ, 189, 441
Gómez-Carrasco, S., & Roncero, O. 2006, JChPh, 125, 054102
González, M., Aguilar, A., & Virgili, J. 1985, CPL, 113, 187
González-Lezana, T., Aguado, A., Paniagua, M., & Roncero, O. 2005, JChPh, 123, 194309
González-Sánchez, L., Vasyutinskii, O., Zanchet, A., Sanz-Sanz, C., & Roncero, O. 2011, Phys. Chem. Chem. Phys., 13, 13656
Gray, S. K., & Balint-Kurti, G. G. 1998, JChPh, 108, 950
Gredel, R. 1997, A&A, 320, 929
Habart, E., Dartois, E., Abergel, A., et al. 2010, A&A, 518, L116
Halvick, P., Stoecklin, T., Larrégaray, P., & Bonnet, L. 2007, PCCP, 9, 582
Harris, H. H., Crowley, M. G., & Leventhal, J. J. 1975, PhRvL, 34, 67
Herbst, E., Champion, R. L., & Doverspike, L. D. 1975, JChPh, 63, 3677
Hierl, P. M., Morris, R. A., & Viggiano, A. A. 1997, JChPh, 106, 10145
Hogerheijde, M. R., Jansen, D. J., & van Dishoeck, E. F. 1995, A&A, 294, 792
Huang, Y., Iyengar, S. S., Kouri, D. J., & Hoffman, D. K. 1996, JChPh, 105, 927
Huang, Y., Kouri, D. J., & Hoffman, D. K. 1994, JChPh, 101, 10493
Jones, C. A., Wendell, K. L., & Koski, W. S. 1977, JChPh, 66, 5325
Joulain, K., Falgarone, E., Pineau des Forets, G., & Flower, D. 1998, A&A, 340, 241
Kessler, M. F., Steinz, J. A., Anderegg, M. E., et al. 1996, A&A, 315, L27
Kroes, G.-J., & Neuhauser, D. 1996, JChPh, 105, 8690
Langer, W. D. 1978, ApJ, 225, 860
Langevin, P. 1905, Ann. Chim. Phys., 5, 245
Larsson, M., & Orel, A. E. 2008, Dissociative Recombination of Molecular Ions (Cambridge: Cambridge Univ. Press)
Le Petit, F., Nehmé, C., Le Bourlot, J., & Roueff, E. 2006, ApJS, 164, 506
Lesaffre, P., Gerin, M., & Hennebelle, P. 2007, A&A, 469, 949
Lesaffre, P., Pineau des Forêts, G., Godard, B., et al. 2013, A&A, 550, A106
Liskow, D. H., Bender, C. F., & Schaefer, H. F. 1974, JChPh, 61, 2507
Mahan, B. H., & Sloane, T. M. 1973, JChPh, 59, 5661
Maier, W. B., II. 1967, JChPh, 46, 4991
Mandelshtam, V. A., & Taylor, H. S. 1995, JChPh, 103, 2903
Marconi, A., Testi, L., Natta, A., & Walmsley, C. M. 1998, A&A, 330, 696
McEwan, M. J., Scott, G. B. I., Adams, N. G., et al. 1999, ApJ, 513, 287
Miller, W. H. 1970, JChPh, 52, 543
Mitchell, J. B. A. 1990, PhR, 186, 215
Naylor, D. A., Dartois, E., Habart, E., et al. 2010, A&A, 518, L117
Pechukas, P., & Light, J. C. 1965, JChPh, 42, 3281
Pellegrini, E. W., Baldwin, J. A., Ferland, G. J., Shaw, G., & Heathcote, S. 2009, ApJ, 693, 285
Pilbratt, G. L., Riedinger, J. R., Passvogel, T., et al. 2010, A&A, 518, L1
Pineau des Forêts, G., Roueff, E., & Flower, D. R. 1986, MNRAS, 223, 743
Plasil, R., Mehner, T., Dohnal, P., et al. 2011, ApJ, 737, 60
Sakai, S., Kato, S., Morokuma, K., & Kusunoki, I. 1981, JChPh, 75, 5398
Saxon, R. P., & Liu, B. 1983, JChPh, 78, 1344
Stoecklin, T., & Halvick, P. 2005, PCCP, 7, 2446
Sullivan, J. P., & Herbst, E. 1978, CPL, 55, 226
Thi, W.-F., Ménard, F., Meeus, G., et al. 2011, A&A, 530, L2
Truhlar, D. G. 1969, JChPh, 51, 4617
van der Tak, F. F. S., Black, J. H., Schöier, F. L., Jansen, D. J., & van Dishoeck, E. F. 2007, A&A, 468, 627
Walmsley, C. M., Natta, A., Oliva, E., & Testi, L. 2000, A&A, 364, 301
Warmbier, R., & Schneider, R. 2011, Phys. Chem. Chem. Phys., 13, 10285
Weselak, T., Galazutdinov, G. A., Musaev, F. A., & Krełowski, J. 2008, A&A, 484, 381
Wesson, R., Cernicharo, J., Barlow, M. J., et al. 2010, A&A, 518, L144
Xie, T., Allen, M., & Langer, W. D. 1995, ApJ, 440, 674
Young Owl, R. C., Meixner, M. M., Wolfire, M., Tielens, A. G. G. M., & Tauber, J. 2000, ApJ, 540, 886
Zamir, E., Levine, R. D., & Bernstein, R. B. 1981, CP, 55, 57
Zanchet, A., Roncero, O., González-Lezana, T., et al. 2009, JPCA, 113, 14488